# Magnetic Phase Diagram of the new Heavy Fermion Compound $Ce_2PtIn_8$

M. Kratochvílová[1], K. Uhlířová[1], J. Custers[1], J. Prokleška[1], and V. Sechovský[1]

[1] *Faculty of Mathematics and Physics, Charles University in Prague, Ke Karlovu 5, 121 16 Prague 2, Czech Republic.*

(Dated: March 4, 2017)

## Abstract

We report on the discovery and investigation of a new 218 heavy Fermion compound. Crystals have been synthesized from In-flux. Structurally, $Ce_2PtIn_8$ is located between the cubic $CeIn_3$ and the more two-dimensional $CeTIn_5$ ($T$ = transition metal) type of compounds. The weak anisotropy of the paramagnetic susceptibility suggests rather 3D magnetic correlations. Specific heat, electrical resistivity and magnetization measurements revealed that $Ce_2PtIn_8$ orders antiferromagnetically below $T_N = 2.1$ K. An order-to-order transition is observed at $T_m = 2$ K. Similarities in the $H - T$ phase diagram to other $Ce_nT_mIn_{3n+2m}$ ($T$ = Rh, Pt) compounds point to a pressure–induced quantum phase transition (QPT) which, according to the tentative location of $Ce_2PtIn_8$ in the recent proposed global phase diagram for QPT, would be of spin density wave type.

PACS numbers: 75.30.Mb,75.30.Kz,75.30.-m,05.30.Rt

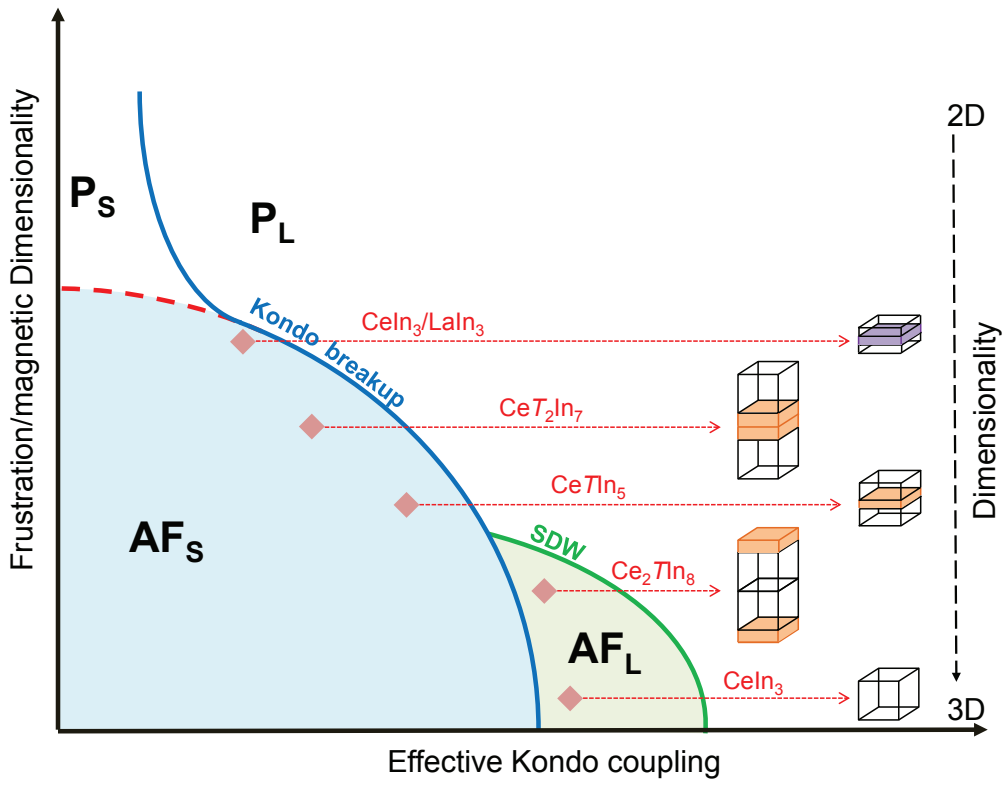


FIG. 1: Tentative location of the $Ce_nT_mIn_{3n+m}$ compounds in the global phase diagram for HF compounds near a zero–$T$ magnetic instability [18, 20]. $AF_L$ ($P_L$): ground state is AFM (is PM) and the Fermi volume includes both, the conduction electrons and local moments. $AF_S$: ground state is AFM (is PM) and the Fermi volume exhibits conduction electrons only.

Heavy fermion (HF) physics covers several central issues in modern physics, like unconventional superconductivity (SC) in condensed matter physics [1, 2], an electronic version of a nematic phase (liquid crystal physics) [3] and quantum phase transitions [4], a topic also heavily debated in astrophysics. Heavy fermion materials are inherently close to a magnetic quantum critical point (QCP). In these materials the Kondo effect, promoting a paramagnetic ground state, competes with the indirect magnetic interaction between localized moments mediated by polarized conduction electrons. The Doniach phase diagram illustrates this rivalry [5]. It plots the effective exchange interaction between the localized moments and the conduction electrons, $J$, versus the (antiferro-)magnetic ordering temperature $T_N$. Initially $T_N$ increases with increasing $J$, passes through a maximum and vanishes at a critical value $J_c$ determining the magnetic QCP – a second-order zero temperature magnetic to non-magnetic phase transition solely driven by critical quantum

fluctuations.

In view of formalisms based on space-time generalization of classical critical phenomena, the transition into the magnetically ordered state originates from a spin-density-wave (SDW) instability [6–8]. By contrast, the local moment (or Kondo breakdown) quantum critical scenario (LM), upon approaching from the paramagnetic side, assumes a sudden reconfiguration of the Fermi surface accompanied by a termination of the Kondo effect at the $T = 0$ paramagnetic–magnetic boundary itself [9–13].

However, the Doniach picture of a "single QCP" depending on a single parameter $J$ cannot account for all observations in HF physics. Recent experiments on Yb-based HF compounds reveal the presence of a zero-$T$ non-Fermi liquid (NFL) phase [14–17]. $Yb(Rh_{0.93}Co_{0.07})_2Si_2$ even presents both types of QCPs. Those being a LM QCP residing deep into the antiferromagnetic (AFM) phase and a SDW QCP on the boundary to paramagnetism (PM). [16] Those results, including the discovery of a LM QCP in the cubic compound $Ce_3Pd_{20}Si_6$ [18], evoke the extension of the Doniach phase diagram by a second parameter, $G$ (or $Q$), the magnetic dimensionality/frustration [17–22]).

It is highly necessary to verify this new phase diagram on a series of measurements on a single material where the dimensionality is subsequently changed from 3D to 2D. However, such experiment is difficult to accomplish. An example of this is the tailored $CeIn_3$-$LaIn_3$-compound which can be viewed as a approximate 2D version of $CeIn_3$ (cubic, $T_N \to 0$ at $p_c \approx 2.6$ GPa).

Alternatively, the family of $Ce_nT_mIn_{3n+2m}$ ($n = 1, 2$; $m = 1, 2$; $T$ = transition metal) HF compounds, often simply called "115", "218" and "127", offer a unique possibility to investigate the influence of dimensionality on quantum criticality. A prototype is $CeRhIn_5$ in which the anisotropic crystal structure leads to a quasi-2D electronic and magnetic structure [23]. At ambient pressure $CeRhIn_5$ orders antiferromagnetically at $T_N = 3.8$ K. With applied hydrostatic pressure the AFM state is gradually suppressed and vanishes at $p_{c1} = 1.77$ GPa when $T_N$ equals the superconducting transition temperature $T_c = 1.9$ K [24]. Measurements show that AFM order coexists with superconductivity over a wide range of pressures below $p_{c1}$ and $T_N > T_c$, while above $p_{c1}$ only unconventional SC is found. In the normal state above the SC dome the physical properties reflect NFL behavior hinting to the presence of a LM QCP hidden deep in the SC state. A smooth extrapolation of $T_N(p)$ to $T \to 0$ suggests that AFM order, if existing, would vanish at a QCP at $p_{c2} \approx 2.3$ GPa.

Supporting evidence for this scenario comes from de Haas–van Alphen experiments showing that at $p_{c2}$ in the normal state the quasiparticle mass diverges. A similar $p-T$ phase diagram is present for $CePt_2In_7$ [**?** ].

The $Ce_nT_mIn_{3n+2m}$ compounds crystallize in the tetragonal $Ho_nCo_mGa_{3n+2m}$ structures consisting of $m$ $TIn_2$–layers alternating with $n$–layers of $CeIn_3$ along the $c$-axis. By adding an additional $CeIn_3$ stacking block the structural dimensionality changes from more 2D towards 3D (127 $\rightarrow$ 115 $\rightarrow$ 218). Figure 1 depicts the motivation behind the present work. By investigating a series of $Ce_nT_mIn_{3n+2m}$ with fixed transition metal it is possible to examine the global phase diagram [18, 20] along the vertical (dimension) axis assuming magnetic frustration to increase upon reducing structural dimensionality.

In this work we present first results of a new member in the $Ce_nT_mIn_{3n+2m}$ family. We were able to grow high quality single crystals of the yet unknown material $Ce_2PtIn_8$. The compound can be regarded as an "intermediate step" between the cubic $CeIn_3$ and the tetragonal $CePtIn_5$.

Single crystals with mass of 1 – 3 mg were successfully grown out of indium flux. Microprobe analysis verified good 218 phase homogeneity. Single crystal X-ray diffraction confirmed that $Ce_2PtIn_8$ crystallizes in the $Ho_2CoGa_8$–type structure with lattice parameters $a = 4.699$ Å and $c = 12.185$ Å. The measurements were conducted in commercial PPMS and MPMS instruments. All results presented in this work were obtained from a single sample. It should be mentioned that reproducibility of the specific heat data was confirmed by repeating the experiments on two other samples from a different batch.

Above $\approx$ 150 K, the susceptibility $\chi(T)$ as a function of temperature in magnetic field applied perpendicular ($\perp c$) and along ($\| c$) the crystallographic $c$-axis, respectively, follows Curie–Weiss (C-W) law with values of the effective moment $\mu_{\rm eff}^{\perp c} = 2.23\mu_{\rm B}/Ce^{3+}$ and $\mu_{\rm eff}^{\| c} = 2.38\mu_{\rm B}/Ce^{3+}$ and Weiss temperature of $\theta_p^{\perp c} = -10$ K and $\theta_p^{\| c} = -2$ K. The $\mu_{\rm eff}$ values are slightly reduced in comparison with that of the free-ion $Ce^{3+}$ (2.54 $\mu_{\rm B}$). We attribute it to crystal field splitting of the $J = 5/2$ multiplet of the $Ce^{3+}$ ion. More interesting, the relatively small difference between $\theta_p^{\perp c}$ and $\theta_p^{\| c}$ demonstrates the low magnetocrystalline anisotropy. For comparison, the Weiss temperatures for the 127–analog, $CePt_2In_7$, yield $\theta_p^{\perp c} = -152$ K and $\theta_p^{\| c} = -31$ K showing a much higher anisotropy [27] in agreement with our earlier considerations regarding dimensionality. The negative Weiss temperatures

determined for $Ce_2PtIn_8$, indicate AFM correlations. In both field directions a double structure around $T = 2$ K appears in the low temperature region of the susceptibility. It is plausible that the first anomaly is a manifestation of a transition into a AFM state. Due to the weak signal it is difficult, however, to follow its evolution in field. The second anomaly is better resolvable and slowly shifts to lower temperatures with increasing field.

Figure 2 displays the specific heat ($C/T$) versus temperature $T$ of $Ce_2PtIn_8$ in zero and various applied magnetic fields $\perp c$ (Fig. 2a) and $\parallel c$ (Fig. 2b) $T < 2.7$ K. As can be seen in the figure, in zero field two transitions appear at $T = 2.1$ K and $T = 2$ K. The upper one is of $2^{\text{nd}}$ order and coincides with the kink in $\chi(T)$. The lower one, in contrast, is very sharp and matches with the second feature in $\chi(T)$ (see Fig. 2b, inset). The sharpness suggests that this is a $1^{\text{st}}$ order transition. Such is expected for a transition from SDW to a stable AFM state bearing different order parameter. However, within resolution of our experiment, we could not resolve latent heat. The double structure in zero field is reminiscent to specific heat results of $Ce_2RhIn_8$ and hence in analogy, the upper one is marked as $T_{\text{N}}$, signaling the onset of an AFM state and the lower transition is labeled as $T_m$ [26]. It is to point out, that in $Ce_2RhIn_8$ only $T_{\text{N}} = 2.8$ K is visible in $\chi(T)$ [25]. The entropy associated with the magnetic transitions obtained by integrating the total specific heat as function of temperature equals $\approx 0.2R \ln 2$ per Ce-atom. This is rather low, having in mind that the value includes the electronic, the magnon and the lattice contribution. The value, even lower than what is found in the sister compound $Ce_2RhIn_8$ being $0.3R \ln 2$ (only electronic part) [26], suggests that Kondo interactions substantially reduce the staggered magnetic moment. Because $La_2PtIn_8$ was not to our disposal (attempts to synthesize failed), we could not separate phonon from magnon ($\beta_m T^2$) contribution. Due to this constrain, we can only determine an order of magnitude for the electronic and phonon contribution. A simple $C/T = \gamma + \beta T^2$ fit was utilized (fit interval: 5 K $< T <$ 10 K). The values yield $\gamma \approx 750$ mJ mol$^{-1}$ K$^{-2}$, qualifying $Ce_2PtIn_8$ as a HF compound, and $\beta = 7.2$ mJ mol$^{-1}$ K$^{-4}$ which corresponds to a Debye temperature of $\Theta_{\text{D}} = 65$ K. The later value is exceptionably low, indicating the need for a proper reference material to subtract the phonon part.

By applying a magnetic field in the *ab*–plane the upper transition $T_{\text{N}}$ remains practically unaffected as displayed the inset in Fig. 2a, whereas $T_m$ gradually shifts to lower $T$. The situation is different if $\mu_0 H \parallel c$. For $\mu_0 H < 1$ T both transitions show no shift

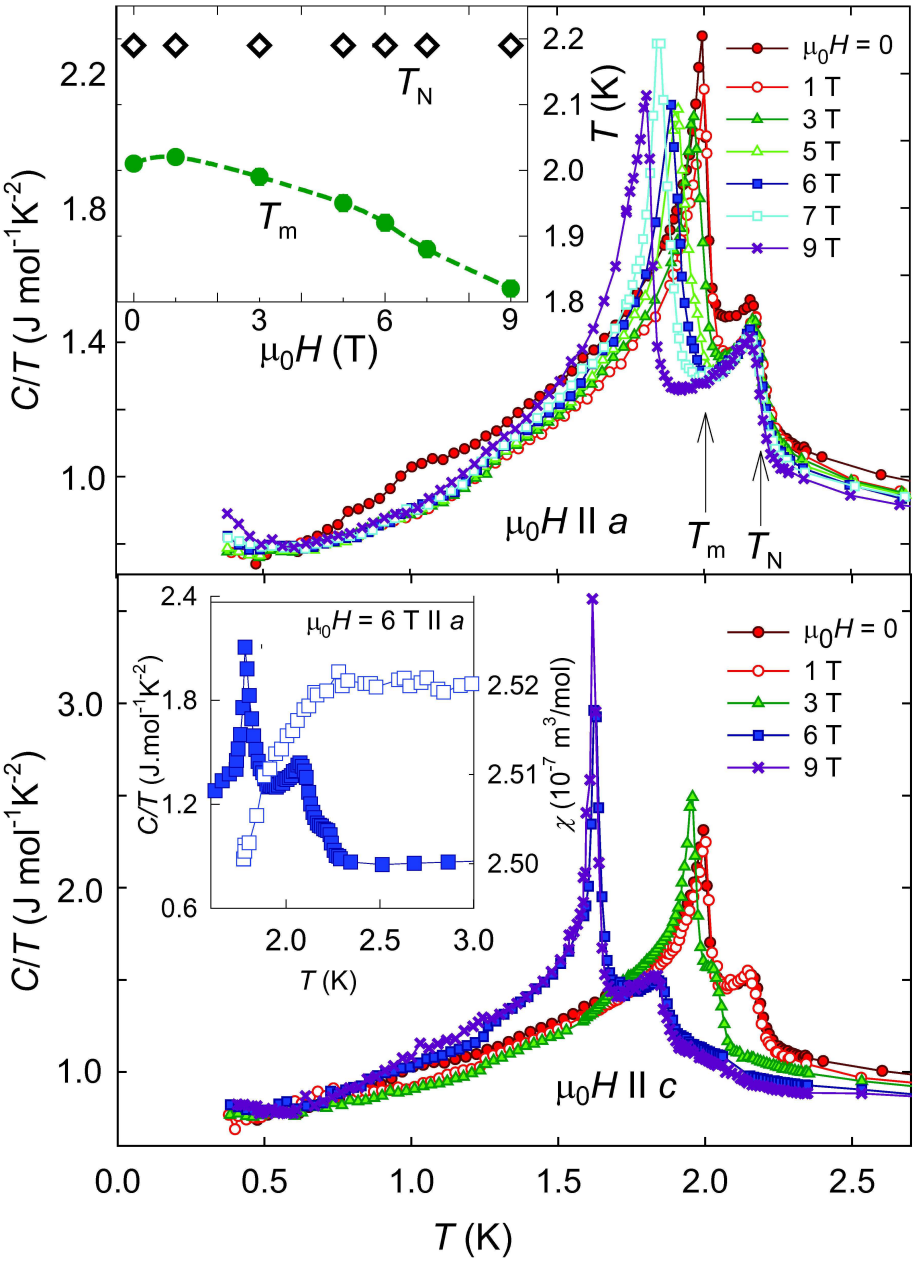


FIG. 2: Specific heat as function of temperature in fields (a) $\perp c$) and (b) $\parallel c$. Inset in (a) shows the evolution of $T_{\rm N}$ and $T_m$ with field applied $\perp$ $c$. Inset (b): a comparison of low-$T$ of $C/T$ ($\mu_0 H \perp c$) with susceptibility data. Dashed lines show position of $T_{\rm N}$ and $T_m$.

in temperature. At slightly higher fields, the upper transition decreases, while $T_m$ stays unchanged. The transitions nearly merge at $\mu_0 H \approx 4$ T before a steep decrease of $T_m$ sets in. In fields greater than 6 T, $T_{\rm N}$ and $T_m$ almost saturate at constant values of $\approx 1.85$ K and $\approx 1.63$ K, respectively.

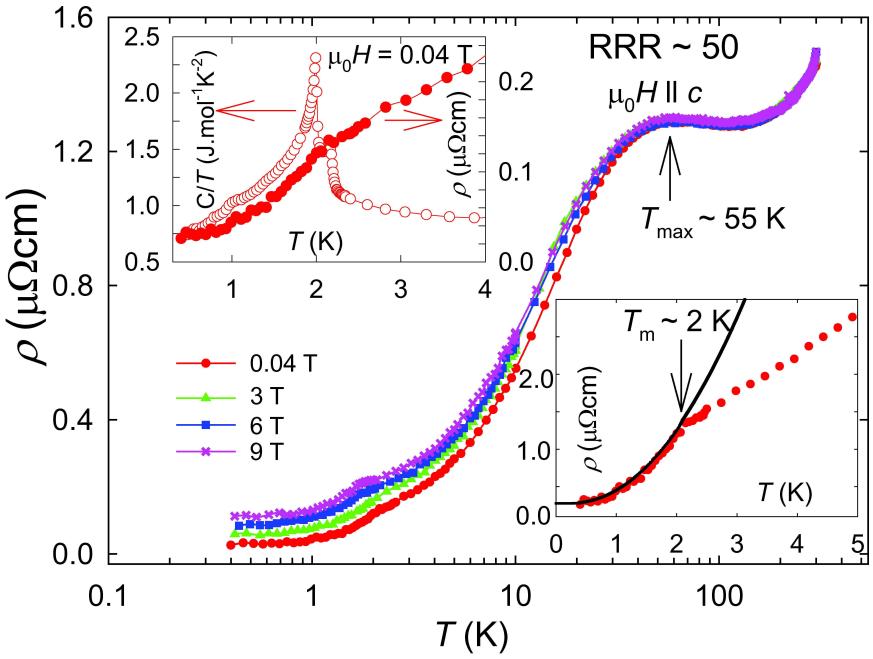


FIG. 3: Temperature dependence of the $c$-axis resistivity ($j \perp c$)in various fields $\parallel c$. The inset shows the low-$T$ $R/R_{300}$ vs. $T$ in $\mu_0 H = 0.04$ T in more detail. The solid line represents a fit of the equation $\rho = \rho_0 + bT[1 + 2T/\Delta]\exp(-\Delta/T) + AT^2$ to the data with parameters $\rho_0$, $b$, $\Delta$ and $A$ that are given in the text.

The resistivity measurement has been conducted with the current flowing in the basal plane. Magnetic fields were applied along the $c$-axis. The results are given in Fig. 3. For clarity, only data of $\mu_0 H = 0.04$, 3, 6 and 9 T are plotted. The small field of $\mu_0 H = 0.04$ T is necessary in order to suppress superconductivity originating from residues of In flux, which in this type of systems is hardly avoidable. Since the transitions in $Ce_2PtIn_8$ are rather robust against magnetic field results will not differ from a real zero field measurement. The residual resistivity ratio ($RRR$) of $\approx 50$ indicates good crystal quality. From Fig. 3 it can be seen that in the PM region the $T$-variation of the resistivity follows a weak temperature dependence with a local maximum at $T_{\rm max} \approx 55$ K marking the crossover from incoherent to coherent Kondo state. Below $T_{\rm max}$ the resistivity drops rapidly. This behavior is typical for Kondo systems, and has been reported for other $Ce_nT_mIn_{3n+m}$ compounds, notably

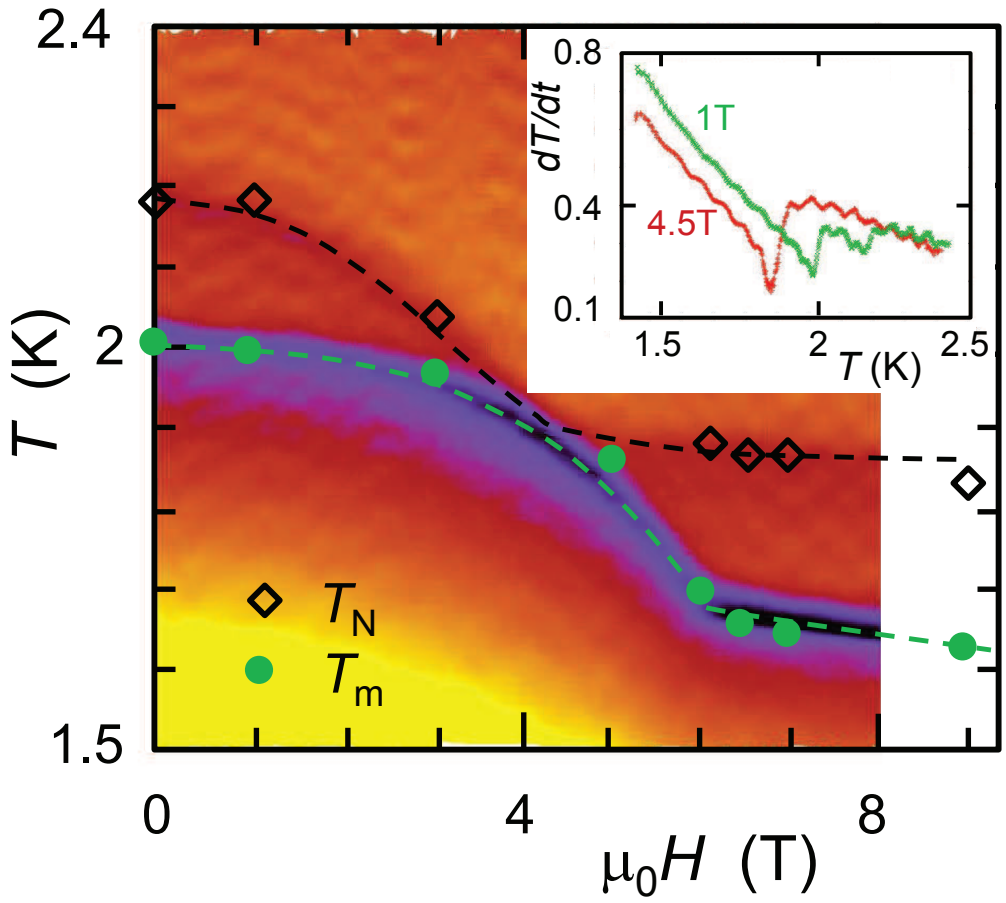


FIG. 4: Phase diagram of the $Ce_2PtIn_8$ for $\mu_0 H \parallel c$ (see text). The diamonds and circles show $T_N$ and $T_m$, respectively, obtained in Fig. 2b. Dashed lines are guide to the eyes.

$Ce_2PdIn_8$ ($T_{max} \approx 60$ K) [28] and $Ce_2RhIn_8$ ($T_{max} \approx 5$ K) [29]. There is an abrupt decrease in $\rho$ at $T \approx 2$ K. The position equals with $T_m$ in specific heat (see Fig. 3, upper inset), whereas $T_N$ is not visible in resistivity. An excellent fit to the data below $T = 2$ K can be achieved using the sum of an expression appropriate for an AFM with an energy gap and a $T^2$–term rejecting Fermi-Liquid (FL) behavior [30]. The parameters $\rho_0 = 0.268$ $\mu\Omega$cm, $b = 0.227 \mu\Omega\text{cm/K}^1$, $\Delta = 1.75$ K and $A = 0.0731 \mu\Omega\text{cm/K}^2$ were obtained from the fit. Obviously the FL contribution is very small. In fields, the resistivity drop moves to lower temperatures mimicking the field dependency of the $T_m$–anomaly in $C/T$.

In order to obtain a detailed view of the $H - T$ phase diagram for $\mu_0 H \parallel c$ ($C/T$ experiments around 4 T were unsuccessful even after several attempts) we performed mapping of the thermal response to the heat pulse. By this method a heat pulse resulting

in a $\Delta T = 1$ K temperature change of the sample (mounted quasi-adiabatically) to the bath temperature $T_{\rm bath}$ was applied. The resulting thermalization of the sample temperature to $T$ was monitored over time $t$. The inset in Fig. 4 shows the derivative of such evolution ($dT/t$) in $\mu_0 H = 1$, and 4.5 T. The color plot shows the derivative $d(\Delta T)/dt$ as a function of bath temperature and field (red: small change in $dT/dt$; blue: large change in $d(T)/dt$). As evident from Fig. 4 the two transitions, $T_{\rm N}$ and $T_m$, merge at $\approx$ 4 T and split again in higher fields. In higher fields ($>$ 5 T) the $T_m$ anomaly sharpens. Similar is observed in $C/T$ (see Fig. 2). For comparison, we included the transition temperatures deduced from specific heat experiments ($T_{\rm N}$: diamonds, $T_m$: circles).

The behavior of $Ce_2PtIn_8$ in magnetic fields resembles some typical observations reported for other $Ce_nT_mIn_{3n+2m}$ members undergoing an AFM transition. Focussing on the $H-T$ phase diagram for fields applied $\perp c$, within our experimental range $T_{\rm N}$ for is robust against magnetic fields. Such robustness is also found in $CePt_2In_7$. Here, $T_{\rm N}$ equals 5.5 K in the entire field range measured (up to 9 T) [27]. In $CeRhIn_5$ and $Ce_2RhIn_8$ $T_{\rm N}$ displays only a marginal shift with field [23]. Interestingly, in the case of $CeRhIn_5$ $T_{\rm N}$ increases contrary to decreasing $T_{\rm N}$ in the 218 compound. The second transition, $T_m$, is more of a mystery. In $Ce_2PtIn_8$, $T_m$ is present in zero field and decreases gradually with increasing field. In the 127–counterpart no second (lower) phase transition is found, whereas in the $CeRhIn_5$ and $Ce_2RhIn_8$ a similar $T_m$-type of transition emerges in applied field. Notably, in both, 115 and 218 Rh–compound, this lower transition (referred to as $T_1$) is of $1^{st}$ order and moves to higher temperatures in larger fields and in the case of $Ce_2RhIn_8$ even merges with $T_{\rm N}$ at $\mu_H \approx 10$ T. In addition, both Rh–compounds exhibit a third transition, $T_2$, that is also magnetic field induced but not observed in $Ce_2PtIn_8$. $T_2$ is situated in between $T_{\rm N}$ and $T_1$ marks transformation into a commensurate state. The transition is only present in a very small field interval and seems to emanate out of $T_{\rm N}$ at low field, decreases with temperature in higher fields and fuses with $T_1$ [23]. One might speculate that $T_m$ in $Ce_2PtIn_8$ corresponds to $T_1$ in the Rh-compounds because of similar field dependence. Hence, one would expect a third transition to appear at even lower temperatures. In analogy to $CeRhIn_5$, the evolution of magnetic order in $Ce_2PtIn_8$ upon lowering $T$ would be: PM $\xrightarrow{T_{\rm N}}$ incommensurate AFM $\xrightarrow{T_m}$ incommensurate AFM. An incommensurate ground state was advanced for $CePt_2In_7$ too [27]. If however, $T_m$ in $Ce_2PtIn_8$, is the analog to $T_2$ in $CeRhIn_5$ then: PM $\xrightarrow{T_{\rm N}}$ incommensurate

AFM $\xrightarrow{T_m}$ commensurate AFM, i. e. , the ground state of $Ce_2PtIn_8$ would be a commensurate AFM state. Neutron experiments are planned to resolve this issue.

To conclude, we have synthesized and characterized single crystal samples of $Ce_2PtIn_8$, a new member of the $Ce_nT_mIn_{3n+2m}$ group. It was found that this HF compound ($\gamma \approx 750$ mJ mol$^{-1}$Ce K$^{-2}$) orders AFM below $T_N$ and undergoes further transition at $T_m$. $Ce_2PtIn_8$, follows the general trend observed in the $Ce_nT_mIn_{3n+2m}$ compounds, i. e. , the AFM transition temperature is lower ($T_N = 2.1$ K) in comparison to its structural more 2D sister $CePt_2In_7$ ($T_N = 5.5$ K). Moreover, magnetization confirms the 3D character of this compound, placing $Ce_2PtIn_8$ close to cubic $CeIn_3$ in the global phase diagram. To reach the magnetic QCP pressure needs to be applied. From the point of view of dimensionality it likely will be a SDW type of quantum phase transition.


[1] P. Coleman, A. J. Schofield, Nature **433,** 226 (2005).

[2] F. Levy, *et al.,* Nature Phys. **3,** 460 (2007).

[3] R. A. Borzi *et al.,* Science **315,** 214 (2007).

[4] H. von Löhneysen *et al.,* Rev. Mod. Phys. **79,** 1015 (2007).

[5] S. Doniach, Physica B **91,** 231 (1977).

[6] J. Hertz, Phys. Rev. B **14,** 1165 (1976).

[7] A. J. Millis, Phys. Rev. B **48,** 7183 (1993).

[8] T. Moriya and K. Ueda, Adv. Phys. **49,** 555 (2000).

[9] P. Coleman *et al.,* J. Phys. Condens. Matter **13,** R723 (2001).

[10] Q. Si *et al.,* Nature **413,** 804 (2001).

[11] T. Senthil, M. Vojta, and S. Sachdev, Phys. Rev. B **69,** 035111 (2004).

[12] T. Senthil *et al.,* Science **303,** 1490 (2004).

[13] C. Pèpin, Phys. Rev. Lett. **98,** 206401 (2007).

[14] S. L. Budko, E. Morosan, and P. C. Canfield, Phys. Rev. B **69,** 014415 (2004).

[15] S. Nakatsuji et al., Nature Phys. **4,** 603 (2008).

[16] S. Friedemann *et al.,* Nature phys. **5,** 465 (2009).

[17] J. Custers *et al.,* Phys. Rev. Lett. **104,** 186402 (2010).

[18] J. Custers *et al.,* Nature Mat. **11,** 189 (2012).

[19] S. Burdin, D. R. Grempel, and A. Georges, Phys. Rev. B **66,** 045111 (2002).

[20] Q. Si, Physica B, **378380,** 23 (2006).

[21] E. Lebanon and P. Coleman, Phys. Rev. B **76,** 085117 (2007).

[22] T. T. Ong and B. A. Jones, Phys. Rev. Lett. **103,** 066405 (2009).

[23] A. L. Cornelius *et al.,* Phys. Rev. B **62,** 14181 (2000).

[24] H. Hegger *et al.,* Phys. Rev. Lett. **84,** 4986 (2000).

[25] P. G. Pagliuso *et al.,* Phys. Rev. B **66,** 054433 (2002).

[26] A. Malinowski *et al.,* Phys. Rev. B **68,** 184419 (2003).

[27] P. H. Tobash *et al.,* J. Phys.: Condens. Matter **24,** 015601 (2012).

[28] D. Kaczorowski *et al.,* Phys. Rev. lett. **103,** 027003 (2009).

[29] S. Ohara *et al.,* Physica B **329–333,** 612 (2003).

[30] N. H. Andersen, in *Crystalline Electric Field and Structural Effects in f-electron Systems,* edited by J. E. Crow, R. P Guertin, and T. W. Mihalisin (Plenum, New York, 1980), p. 373.